Analysis of absolute amounts of two meiotic cohesin subunits, RAD21L and REC8, in mouse spermatocytes

Taniuchi, Yuto ; Hiraide, Kazutaka ; Su, Rilige ; Ijuin, Kazune ; Wei, Xingqiang ; Horii, Takuro ; Hatada, Izuho ; Lee, Jibak

(Citation)
Journal of Reproduction and Development,69(2):78-86

(Issue Date)
2023

(Resource Type)
journal article

(Version)
Version of Record

(URL)
https://hdl.handle.net/20.500.14094/0100481922

Journal of Reproduction and Development, Vol. 69, No 2, 2023

Original Article

Analysis of absolute amounts of two meiotic cohesin subunits, RAD21L and REC8, in mouse spermatocytes

Yuto TANIUCHI[1)*], Kazutaka HIRAIDE[1)*], Rilige SU[1)], Kazune IJUIN[1)], XingQiang WEI[1)], Takuro HORII[2)], Izuho HATADA[2, 3)] and Jibak LEE[1)]

[1)]*Laboratory of Developmental Biotechnology, Graduate School of Agricultural Science, Kobe University, Kobe 657-8501, Japan*
[2)]*Laboratory of Genome Science, Biosignal Genome Resource Center, Institute for Molecular and Cellular Regulation, Gunma University, Gunma 371-8512, Japan*
[3)]*Viral Vector Core, Gunma University Initiative for Advanced Research (GIAR), Gunma 371-8511, Japan*

Abstract. RAD2lL and REC8, meiosis-specific paralogs of the canonical cohesin subunit RAD21, are essential for proper formation of axial/lateral elements of the synaptonemal complex, synapsis of homologous chromosomes, and crossover recombination in mammalian meiosis. However, how many meiotic cohesins are present in germ cells has not been investigated because of the lack of an appropriate method of analysis. In the present study, to examine the intracellular amount of meiotic cohesins, we generated two strains of knock-in (KI) mice that expressed a 3×FLAG-tag at the C-terminus of RAD21L or REC8 protein using the CRISPR/Cas9 genome editing system. Both KI mice were fertile. Western blot analyses and immunocytochemical studies revealed that expression levels and localization patterns of both RAD21L-3×FLAG and REC8-3×FLAG in KI mice were similar to those in wild-type mice. After confirming that tagging of endogenous RAD21L and REC8 with 3×FLAG did not affect their expression profiles, we evaluated the levels of RAD21L-3×FLAG and REC8-3×FLAG in the testes of 2-week-old mice in which only RAD21L and REC8 but little RAD21 are expressed in the meiocytes. By comparing the band intensities of testicular RAD21L-3×FLAG and REC8-3×FLAG with 3×FLAG-tagged recombinant proteins of known concentrations in western blot analysis, we found that there were approximately 413,000 RAD21L and 453,000 REC8 molecules per spermatocyte in the early stages of prophase I. These findings provide new insights into the role played by cohesins in the process of meiotic chromosome organization in mammalian germ cells.
Key words: Cohesin, Germ cell, Meiosis, RAD21L, REC8

(**J. Reprod. Dev. 69:** 78–86, 2023)

Germ cells undergo meiosis, a special type of cell division, to yield genetically variable haploid gametes. Meiosis involves two successive divisions that occur following pre-meiotic DNA synthesis. In meiosis I, homologous chromosomes find their partners and associate with each other through the meiotic events so-called synapsis and crossover recombination. Synapsis is mediated by the synaptonemal complex, which is composed of two proteinaceous axes called axial/lateral elements (AEs/LEs), connected by transverse filaments [1]. Simultaneously, recombination is initiated by Spo11-induced strand breaks, some of which are ultimately repaired, resulting in crossovers [2]. Although synapsis is dissolved at the diplotene stage in prophase I, the chiasmata remain after the crossover recombination is accomplished and contributes to connecting the homologous chromosomes cooperatively with sister chromatid cohesion distal to the chiasmata until the end of metaphase I [3]. During anaphase I, homologous chromosomes separate from each other by the dissolution of sister chromatid cohesion along the chromosome arms while sister chromatids remain attached at the centromeres.

Received: June 14, 2022
Accepted: January 2, 2023
Advanced Epub: February 3, 2023

Correspondence: J Lee (e-mail. leej@tiger.kobe-u.ac.jp)
* Y Taniuchi and K Hiraide contributed equally to this work.

Cohesin is a multi-subunit protein complex that consists of SMC1α, SMC3, RAD21, and either SA1/STAG1 or SA2/STAG2 in proliferating vertebrate cells [4, 5]. Cohesin can form a ring-shaped structure, and thus, is thought to mediate sister chromatid cohesion by embracing the two DNA molecules of the sister chromatids in a single ring or by linking two rings, each of which traps one of the sister DNAs [6–8]. Cohesin also organizes interphase chromatin by forming chromatin loops and topologically associating domains (TADs) with the help of CTCF, the chromatin-colocalizing partner of cohesin that is involved in the regulation of gene expression [9–11]. In addition to canonical subunits, mammalian germ cells express several meiosis-specific subunits: SMC1β (SMC1α paralog) [12], STAG3 (SA/STAG subunit paralog) [13], and REC8 [14, 15] and RAD21L (RAD21 paralogs) [16–18] (Fig. 1A). These meiosis-specific cohesin subunits are localized along the AEs/LEs of the synaptonemal complex in some stages of prophase I, and are essential for proper axial element formation, synapsis of homologous chromosomes, and crossover recombination [19, 20]. Depletion of any one of the meiosis-specific subunits causes meiotic arrest at the leptotene-like or zygotene-like stage in spermatocytes. *Rec8*-null spermatocytes are arrested at the zygotene-like stage with impaired synapsis and modest defects in axial element formation [21, 22]. *Rad21L*-null spermatocytes are also arrested at the zygotene-like stage due to impaired synapsis and recombination along with shortened AEs, although RAD21L-deficient female mice are fertile but show age-dependent infertility [23]. However, *Rec8*/*Rad21L* double knock-out (KO) mice showed a severe phenotype as the AEs failed to assemble

in meiocytes [24]. Furthermore, a study using several strains of KO mice demonstrated that the initial pairing of homologous chromosomes is dependent on RAD21L but not REC8 [25]. Despite advances in our understanding of intracellular functions, no data are available on the intracellular quantity of meiotic cohesins. It is widely thought that meiosis-specific subunits play special roles in meiocytes because they are qualitatively different from the canonical subunits. For now, however, it is undeniable that the amount of meiotic cohesins is so high in meiocytes that they may play some of the specific roles. Therefore, it is important to determine the quantity of meiotic cohesins to understand the regulatory mechanisms of chromosome dynamics. It has been suggested that meiotic cohesins are also involved in the regulation of gene expression [26, 27], and determining the quantity of meiotic cohesins is important for understanding the regulation of gene expression in germ cells.

In general, western blot analysis is not conducted to compare the amounts of different proteins because the extent of reactivity differs among antigen-antibody complexes. In this study, to circumvent this problem, we developed knock-in (KI) mice that expressed a 3×FLAG-tag at the C-terminal end of RAD21L or REC8 protein. These proteins could be detected using the same anti-3×FLAG antibodies, which enabled us to compare the relative expression levels of different proteins by western blot analysis. Furthermore, this is the first study in which the absolute amount of meiotic cohesins in mammalian germ cells was determined using a recombinant 3×FLAG-tagged protein of known concentration as a standard in western blot analysis.

Materials and Methods

Production of Rec8-3×Flag and Rad21L-3×Flag knock-in (KI) mice

We developed *Rec8-3×Flag* and *Rad21L-3×Flag* KI mice by genome editing using the clustered regularly interspaced short palindromic repeats (CRISPR)-Cas9 system, as described previously [28]. The design of the KI mice is shown in Supplementary Figs. 1 and 2. In brief, C57BL/6J female mice were induced to superovulate by injecting 7.5 units of equine chorionic gonadotropin (eCG; ASKA Pharmaceutical, Tokyo, Japan); 48 h later, the mice were administered 7.5 units of human chorionic gonadotropin (hCG; ASKA Pharmaceutical). After hCG administration, the females were mated with the C57BL/6J males. Zygotes were isolated from the oviduct 21 h later. After washing in M2 medium (Sigma-Aldrich, St. Louis, MO, USA), the zygotes were incubated in few drops of M16 medium (Sigma-Aldrich) supplemented with penicillin and streptomycin at 37°C. Electroporation was conducted using the simultaneous method 24–27 h post-hCG administration. The fertilized eggs were electroporated with recombinant Cas9 protein (100 ng/μl; GeneArt Platinum™ Cas9 Nuclease, Thermo Fisher Scientific, Waltham, MA, USA), CRISPR RNAs (crRNAs) and trans-activating CRISPR RNAs (tracrRNAs; 34 ng/μl; IDT, Coralville, IA, USA), and single-stranded oligodeoxynucleotides (ssODNs; 400 ng/μl; IDT). After culture, 2-cell embryos were transferred to the oviduct of pseudopregnant females. Consequently, 19 and 17 pups were obtained for *Rec8-3×Flag* and *Rad21L-3×Flag* KI, respectively. These mice were subjected to primary screening for *3×Flag* KI by conducting PCR and *Eco*RV digestion of the PCR products. The primer sets used for amplification of *Rec8* and *Rad21L* were as follows: *Rec8* forward primer, 5′-TTCTGACCAGTGCTGTCCAC-3′; *Rec8* reverse primer, 5′-AGATGTGCAAGGGAATGAGG-3′; *Rad21L* forward primer, 5′-AAAACATCGTGCTATTGAGCTG-3′; and *Rad21L* reverse primer, 5′-ACCATCAGCTGCTTCCAGAT-3′. The genotypes were confirmed by DNA sequence analysis after TA cloning using the pGEM-T Easy vector system. A mouse with a *3×Flag* DNA insertion in one allele without undesirable indels was used for the generation of KI mice. By mating the mice with wild-type mice, hetero KI mice were obtained. To ensure that the progeny had an accurate *3×Flag* insertion, the genotypes were examined by sequence analysis.

Male and female mice of wild-type, *Rad21L-3×Flag* homo KI, and *Rec8-3×Flag* homo KI strains aged 3 months or older, but less than 7 months, were mated to examine the litter sizes of these mice. Statistical analyses were conducted using Bell Curve for Excel (version 3.21, Social Survey Research Information Co., Ltd., Tokyo, Japan), an add-in software for the Japanese version of Microsoft Excel. The means of litter sizes were statistically evaluated by Welch's t-test, and a P value < 0.05 was considered statistically significant.

This study was approved by the Institutional Animal Care and Use Committee (permission number: 2019-05-07) and carried out according to the Kobe University Animal Experimentation Regulations. This study was also approved by the Committee for Safe Handling of Living Modified Organisms in Kobe University (permission numbers: 29-70 and 2019-09) and was carried out according to the Guidelines of the Committee.

Preparation of testis extracts

Mouse testis extracts were prepared according to the method described previously [18]. Testes were collected from 14.5-day-old or 8-week-old mice, homogenized with a pestle, and sonicated in TNE buffer (20 mM Tris-HCl [pH 7.4], 150 mM NaCl, 2 mM EDTA, 1% [v/v] Nonidet P-40, 50 mM NaF, and 1 mM Na_3VO_4) supplemented with a protease inhibitor cocktail (cOmplete mini EDTA-free; Merck, Darmstadt, Germany). After centrifugation at 20,000 *g* for 30 min at 4°C, the supernatant was collected as the testis extract. To prepare the sample for sodium dodecyl sulfate-polyacrylamide gel electrophoresis (SDS-PAGE), an equal volume of 2×SDS sample buffer (250 mM Tris-HCl [pH 6.8], 4% [w/v] SDS, 40% [v/v] glycerol, 100 mM dithiothreitol, and 0.02% [w/v] bromophenol blue) was added to the extract; the mixture was boiled for 3 min and stored at –20°C until use.

Sodium dodecyl sulfate-polyacrylamide gel electrophoresis (SDS-PAGE), western blotting, and phosphatase treatment

The samples were electrophoresed using a 7.5% acrylamide gel and then transferred to a PVDF membrane (Thermo Fisher Scientific) with a Trans-Blot Turbo Transfer System (Bio-Rad Laboratories, Inc., Hercules, CA, USA). The membranes were blocked in blocking buffer (1% bovine serum albumin in TBST [20 mM Tris-HCl, 150 mM NaCl, and 0.1% Tween 20; pH 7.5]) for 30 min and then incubated with primary antibodies at 1 μg/ml final concentration in the blocking buffer overnight at 4°C. The primary antibodies used for western blotting were anti-RAD21L [18], anti-REC8 [15], anti-SMC3 (ab9263-50, Abcam, Cambridge, UK), and anti-3×FLAG, as described below. After washing three times with TBST, the membranes were incubated with horseradish peroxidase-labeled anti-rabbit IgG secondary antibodies (Cytiva, Tokyo, Japan). The antigen-antibody complexes were detected by incubation with ECL Prime Western Blotting Detection Reagent (Cytiva) and observed using Image Saver 6 (ATTO, Tokyo, Japan). The intensity of the band obtained in the western blot was used for quantification using the ImageJ software.

To compare the band intensities of wild-type and 3×FLAG-tagged REC8 extracted from the heterozygous KI mouse testes, the REC8

protein was treated with λ-protein phosphatase (λ-PPase; New England BioLabs, Ipswich, MA, USA) to prevent overlap between the bands of phosphorylated wild-type REC8 and 3×FLAG-tagged REC8 in the western blot. For the treatment of REC8 with λ-PPase, immunoprecipitates obtained with anti-REC8 antibody and protein A Sepharose (Cytiva) were washed five times in TNE buffer, twice in 1× λ-PPase buffer supplied with λ-PPase, and then incubated with 20 U/μl λ-PPase for 30 min at 37°C. After washing with 1× λ-PPase buffer, the immunoprecipitates were eluted by boiling in 1× SDS sample buffer for 3 min and subjected to western blot analysis. To compare the band intensities of wild-type and 3×FLAG-tagged RAD21L extracted from heterozygous KI mouse testes, similar experiments were conducted using anti-RAD21L antibody for immunoprecipitation (without λ-PPase treatment).

Preparation of anti-3×FLAG antibody

Custom peptide synthesis and custom antiserum production services (Hokkaido System Science, Sapporo, Japan) were utilized for the production of anti-3×FLAG antibody. The 3×FLAG peptides (C-DYKDHDGDYKDHDIDYKDDDDK) were synthesized and conjugated to keyhole limpet hemocyanin (KLH). The 3×FLAG peptides conjugated with KLH were used as antigens to immunize rabbits. The obtained antisera were affinity-purified with 3×FLAG peptide-conjugated SulfoLink Coupling Resin (Thermo Fisher Scientific) to produce an anti-3×FLAG antibody.

Preparation of C-terminal partial REC8-3×FLAG recombinant protein

A previously constructed pET21c plasmid vector, into which cDNA encoding carboxy-terminal partial mouse REC8 was inserted [15], was digested by *Xho*I (Nippon Gene, Tokyo, Japan). Annealed oligo DNAs encoding 3×FLAG (Forward: 5′-TCGAGGACTACAAGG ATCATGATGGCGACTACAAGGATCATGATATCGACTAC AAGGATGACGATGACAAGTGA-3′, Reverse: 5′-TCGATCACT TGTCATCGTCATCCTTGTAGTCGATATCATGATCCTTGT AGTCGCCATCATGATCCTTGTAGTCC-3′ [the underlined sequences are complementary to the protruding ends created by *Xho*I digestion]) were inserted into the *Xho*I-digested site of the vector. The constructed vector was transformed into Rosetta 2 (DE3)-competent cells (Sigma-Aldrich). Recombinant protein expression was induced by incubating *Escherichia coli* with 1 mM isopropyl-β-D-thiogalactopyranoside (Takara Bio, Kusatsu, Japan) for 3 h. The recombinant proteins were purified from inclusion bodies by electroelution. Briefly, the inclusion bodies were resuspended in a solution (pH 8.0) containing 300 mM NaCl, 50 mM sodium phosphate, and 10% glycerol, lysed by adding an equal volume of 2× SDS sample buffer, and boiled for 3 min. The extracted proteins were separated by SDS-PAGE and stained with Coomassie Brilliant Blue. The recombinant protein with a predicted molecular weight of 43.3 kDa was removed from the gel and purified by electroelution. The electroelution was conducted in cellulose tubes (Sanko Junyaku Co., Ltd., Tokyo, Japan) filled with an electroelution buffer (100 mM sodium phosphate and 0.1% SDS; pH 7.0) at 100 V and 100 mA for 17 h. The recombinant protein was concentrated using an Amicon Ultra-0.5 Device (10 kDa cutoff; Merck), and the concentration was calculated using the RC-DC Protein Assay kit (Bio-Rad Laboratories) according to the manufacturer's instructions.

Immunocytochemistry of nuclear spreads

Nuclear spreads were prepared, fixed, and immunofluorescently labeled according to the method described previously [15]. Rabbit polyclonal anti-RAD21L antibody [18], rabbit polyclonal anti-REC8 antibody [15], and mouse polyclonal anti-SYCP3 antiserum [15] were used as primary antibodies. The primary antibodies were detected with Alexa488 anti-mouse IgG and Alexa568 anti-rabbit IgG secondary antibodies (Thermo Fisher Scientific). DNA was counterstained with 4′,6-diamidino-2-phenylindole dihydrochloride (DAPI; Dojindo Laboratories, Kumamoto, Japan). Images were obtained using a confocal laser scanning microscope (FV1000-KDM; Olympus, Tokyo, Japan).

Calculation of the number of meiotic cells and RAD21L-positive cells in testes of 14.5-day-old mice

Testes were isolated from 14.5-day-old mice, and testicular cell suspensions were prepared according to the previously described method [29]. The numbers of cells in the testes were calculated by counting the cells in the suspension using a hemocytometer. Testes derived from 14.5-day-old mice were cryo-sectioned and fixed as described previously [15]. The sections were immunofluorescently labeled with rabbit polyclonal anti-SYCP3 primary antibody [15] and Alexa568 anti-rabbit IgG secondary antibody (Thermo Fisher Scientific), and DNA was counterstained with DAPI. The ratio of meiotic cells to total cells in the testes was calculated as the ratio of SYCP3-positive to DAPI-positive nuclei. The number of meiotic cells in the testes was calculated by multiplying the total number of cells by the meiotic ratio. Since 14.5-day-old testes may contain late pachytene spermatocytes that do not express RAD21L [30, 31], the sections were also immunofluorescently labeled with rabbit polyclonal anti-SYCP3 antibody and rat polyclonal ant-RAD21L antiserum [18] and detected using Alexa488 anti-rat IgG antibody and Alexa568 anti-rabbit IgG antibody. The ratio of RAD21L-positive cells in SYCP3-positive meiotic cells was then calculated.

Results

Production of KI mice expressing REC8-3×FLAG or RAD21L-3×FLAG

To investigate the intracellular amount of RAD21L and REC8 during mammalian meiosis by western blot analysis (Fig. 1B), we first generated KI mice harboring a DNA sequence encoding the 3×FLAG tag inserted just upstream of the stop codon of *Rec8* or *Rad21L* using the CRISPR/Cas9 genome editing system (Supplementary Figs. 1 and 2). After electroporation of Cas9 protein, crRNAs, tracrRNAs, and donor ssODNs into the embryos, the embryos were transferred to recipient mice. In the case of *Rad21L-3×Flag* KI mice, to increase the efficiency of homology-directed repair during the process of 3×FLAG insertion, the donor ssODN was designed to remove a DNA sequence encoding two amino acids just upstream of the stop codon. Removal of these amino acids did not affect protein expression or function, as expected from the poor conservation of the two amino acid residues among vertebrate orthologs.

Among the obtained pups, which are 17 pups for *Rad21L* and 19 pups for *Rec8*, 2 *Rad21L-3×Flag* and 3 *Rec8-3×Flag* KI mice, respectively, had a 3×FLAG-coding DNA sequence just upstream of the stop codon without undesirable indels. The founder mice were mated with wild-type mice, and subsequently, the hetero KI mice were mated to produce homo KI mice of both strains. Both homozygous *Rad21L-3×Flag* and *Rec8-3×Flag* KI mice were fertile and produced healthy pups. The average litter sizes of *Rad21L-3×Flag* and *Rec8-3×Flag* KI mice were 6.3 and 6.2, respectively, which were not significantly different from that of wild-type mice (6.7; Welch's t-test, P = 0.518 for wild-type and Rad21L KI and P

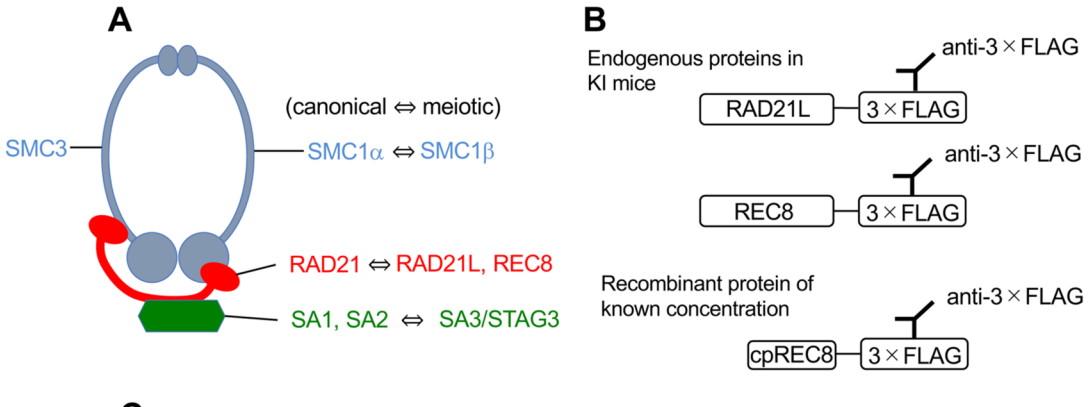

C

	adult testis			
	14.5-day-old testis			
	Mitotically proliferating cells	Meiotic cells		Post-meiotic cells
		before mid- or late-pachynema#	after late-pachynema	
RAD21	+	−	+	+
RAD21L	−	+/−#	−	−
REC8	−	+	+	+

Fig. 1. Overview of the experimental design. (A) Composition of subunits of canonical and meiotic cohesin complexes. SMC3 is a common subunit found in all types of canonical and meiotic cohesins. (B) For quantitative immunoblot analysis, three types of 3×FLAG-tagged proteins were prepared in this study. Endogenous RAD21L-3×FLAG and REC8-3×FLAG were extracted from the testes of two strains of knock-in mice that had been developed by genome editing. The recombinant C-terminal partial REC8-3×FLAG (cpREC8-3×FLAG) was expressed in *Escherichia coli*, purified, and used as a standard for comparison with the endogenous 3×FLAG-tagged proteins. These proteins were detected using anti-3×FLAG antibody in the western blot analysis. (C) Expression patterns of three kleisin subunits (RAD21, RAD21L, and REC8) of cohesin in the testicular cells of 14.5-day-old and adult mice. #) RAD21L is expressed until mid-pachynema stage but not in late-pachynema stage.

= 0.456 for wild-type and Rec8 KI; Supplementary Fig. 3). These results indicated that KI of 3×FLAG-coding DNA into *Rad21L* or *Rec8* did not affect fertility.

Tagging of endogenous RAD21L and REC8 with 3×FLAG did not affect their expression profiles

To confirm the expression of RAD21L-3×FLAG and REC8-3×FLAG proteins in KI mice, we conducted western blot analyses using testes extracts from the wild-type and the two adult KI mice strains (Fig. 2). Immunoblot analysis revealed that levels of SMC3, which is used as an internal control during analysis of all types of cohesins (Fig. 1A), were similar in the testes of wild-type and KI mice (Fig. 2). Analysis using anti-RAD21L and anti-REC8 antibodies revealed that the RAD21L (approximately 95 kDa) and the REC8 (approximately 75 kDa) band intensities were similar for wild-type and the respective KI mice (Figs. 2A and 2B). The bands of proteins obtained from both KI mice were slow-migrating, probably due to the increase in molecular weight caused by the 3×FLAG tags (Figs. 2A and 2B). We also examined whether the 3×FLAG-tagged RAD21L and REC8 were expressed at levels similar to those of the wild-type proteins expressed in the testes of heterozygous KI mice. In both KI samples, bands representing the wild-type and the 3×FLAG-tagged proteins had similar intensities (Fig. 2C). These results indicated that tagging RAD21L and REC8 with the 3×FLAG did not change their protein expression levels. Two bands of sizes 95 and 75 kDa were detected upon immunoblot analysis with anti-3×FLAG antibody using proteins extracted from *Rad21L-3×Flag* and *Rec8-3×Flag* KI mice, respectively, whereas these bands were not detected upon analysis of proteins extracted from the wild-type mice (Fig. 2D), indicating that RAD21L and REC8 were expressed in the 3×FLAG-tagged forms in these KI mice. Notably, the signal intensity of the REC8-3×FLAG band was much higher (about 4.3 times higher on average of two replicates) than that of the RAD21L-3×FLAG band; however, the signal intensities of the SMC3 bands (internal control) were similar in both KI mouse testes, indicating that adult testes contain a higher level of REC8 than that of RAD21L.

Immunofluorescence analyses of nuclear spreads of spermatocytes were conducted to examine whether the 3×FLAG tag affected the localization of REC8 and RAD21L (Figs. 3 and 4). It has been reported that RAD21L localizes along the AEs/LEs from the leptotene to the mid-pachytene stages [18], whereas REC8 does so throughout prophase I [14, 15]. In both wild-type and *Rad21L-3×Flag* KI mouse spermatocytes, RAD21L signals were detected along AEs/LEs during leptotene, zygotene, and some pachytene stages, whereas the signal was hardly detected during the rest of the pachytene and diplotene stages (Fig. 3). In both wild-type and *Rec8-3×Flag* KI mouse spermatocytes and spermatids, REC8 signals were detected along the AEs/LEs throughout prophase I and in the nuclei of the post-meiotic cells (Fig. 4). Thus, tagging of RAD21L and REC8 with the 3×FLAG did not affect their cellular localization.

Judging from the results of western blotting and immunofluorescent analysis, as well as the fertility of KI mice, RAD21L-3×FLAG and

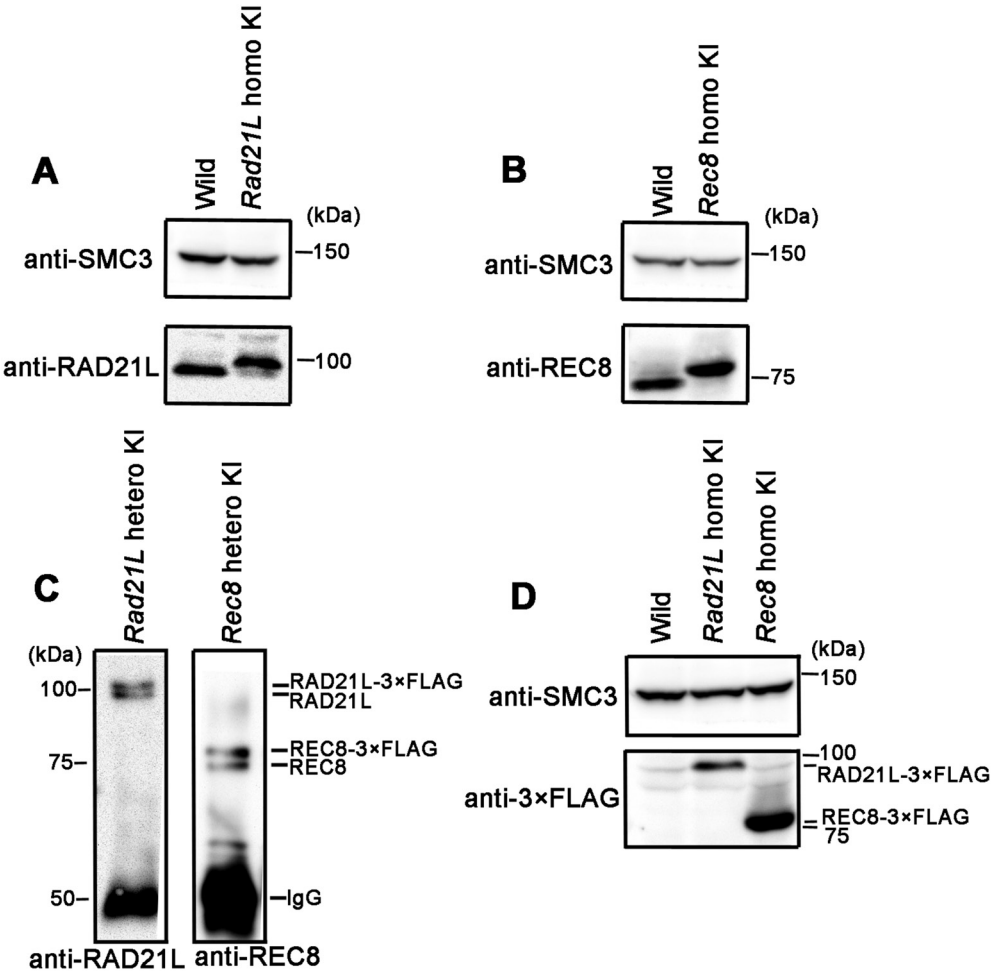

Fig. 2. The expression of RAD21L-3×FLAG and REC8-3×FLAG in testes of two knock-in (KI) mice strains. (A) Immunoblot analysis of testes extracts from wild-type and *Rad21L-3×Flag* homo KI 8-week-old mice using anti-SMC3 and anti-RAD21L antibodies. (B) Immunoblot analysis of testes extracts from wild-type and *Rec8-3×Flag* homo KI 8-week-old mice using anti-SMC3 and anti-RAD21L antibodies. (C) Testes extracts from *Rad21L-3×Flag* hertero KI and *Rec8-3×Flag* hetero KI 8-week-old mice were immunoprecipitated with anti-RAD21L and anti-REC8 antibodies, respectively. Then, only the immunoprecipitates obtained with anti-REC8 antibody was treated with λ-PPase. The anti-RAD21L and anti-REC8 immunoprecipitates were subjected to western blot analyses using anti-RAD21L and anti-REC8 antibodies, respectively. (D) Immunoblot analysis of testes extracts from wild-type, *Rad21L-3×Flag* homo KI, and *Rec8-3×Flag* homo KI 8-week-old mice using anti-SMC3 and anti-3×FLAG antibodies.

REC8-3×FLAG proteins were considered to have the same properties as the wild-type proteins.

Absolute quantitation of RAD21L and REC8 in spermatocytes during early prophase I

After confirming that tagging of 3×FLAG had no effect on the features of both RAD21L and REC8, we conducted western blot analysis to examine the absolute amounts of these proteins in the testes of 14.5-day-old mice (Fig. 5A), which contain spermatocytes that have reached up to the pachytene stage [30, 31]. The use of 14.5-day-old testes offered two advantages. First, determining the amounts of RAD21L and REC8 leads to the determination of the total amount of cohesin in meiocytes because RAD21L and REC8, but hardly RAD21, are expressed in the early stages of prophase I [15, 17, 18]. Second, we can estimate the average numbers of RAD21L and REC8 per meiocyte since most of the meiocytes in 14.5-day-old testes express both RAD21L and REC8, in contrast to adult testes, which contain meiocytes that do not express RAD21L (Fig. 1C). To examine the amounts of RAD21L and REC8 in the same samples, heterozygous *Rad21L-3×Flag*/*Rec8-3×Flag* KI pups were prepared by mating two lines of homozygous KI mice. Using the serially diluted C-terminal partial REC8 (cpREC8)-3×FLAG recombinant protein, which was expressed in *E. coli* so that it could be used as a standard sample (Fig. 1B), a calibration curve was drawn (Fig. 5B). Then, we measured the signal intensities of REC8-3×FLAG and RAD21L-3×FLAG and estimated that a single testis of the heterozygous KI mouse contains 142 ± 13.8 fmol of RAD21L-3×FLAG and 156 ± 26.7 fmol of REC8-3×FLAG (mean ± standard deviation, n = 3; Fig. 3C). By multiplying the number of moles by Avogadro's constant (6.02×10^{23}) and doubling it (considering that two alleles contributed to the gene expression), it is estimated that one testis of a 14.5-day-old mouse contains an average of approximately 1.71×10^{11} RAD21L and 1.88×10^{11} REC8 molecules. To determine the number of meiocytes in a 14.5-day-old testis, we examined the total cell number and meiotic ratio (Supplementary Fig. 4). We found that one testis contained $9.4 \times 10^5 \pm 2.4 \times 10^5$ cells (mean ± standard deviation of 10 testes examined) and the percentage of meiotic cells averaged 44.1% (number of cells examined = 6342). We also observed

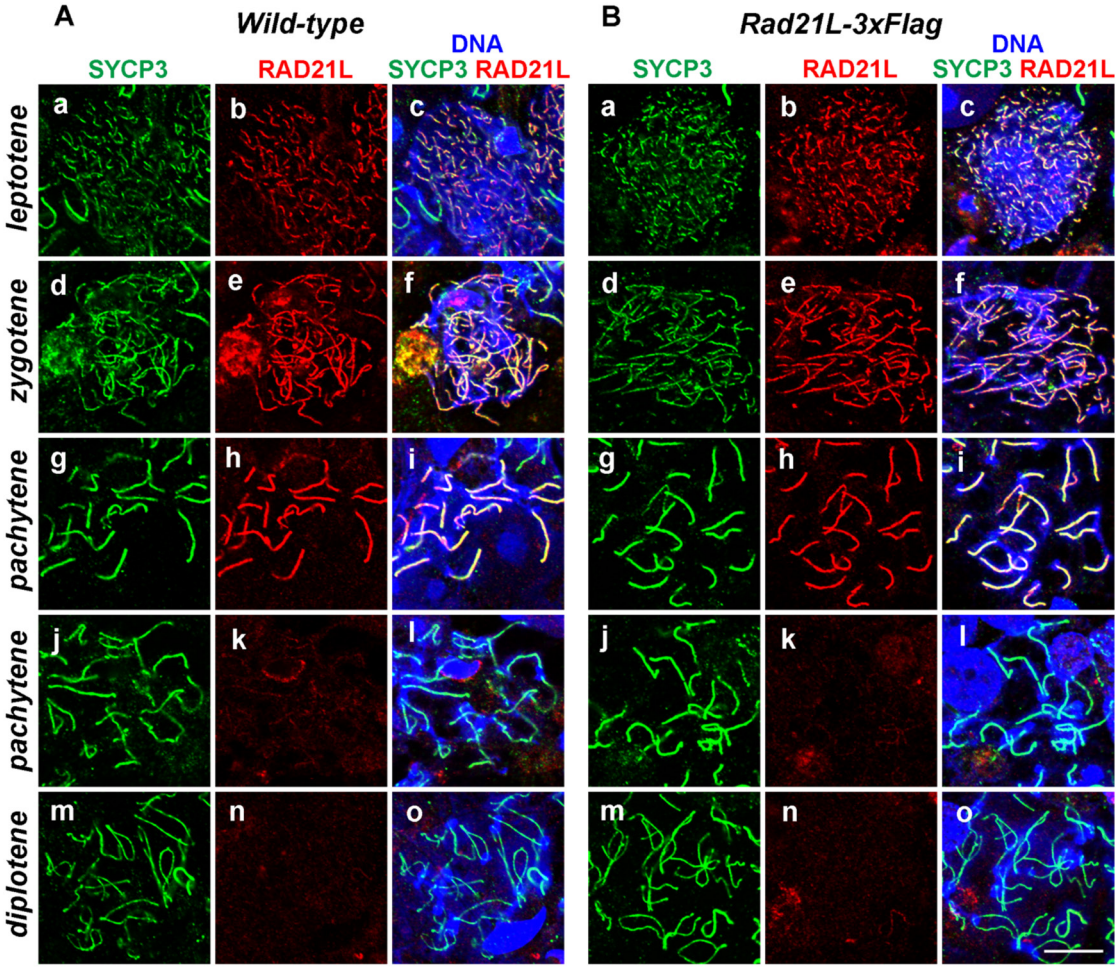

Fig. 3. The localization of RAD21L in nuclear spreads from *Rad21L-3×Flag* KI and wild-type 8-week-old mice. Nuclear spreads of testicular cells from wild-type (A) and *Rad21L-3×Flag* KI (B) 8-week-old mice were prepared and immunofluorescently labelled with anti-RAD21L and anti-SYCP3 antibodies. The DNA was counterstained with DAPI. Spermatocytes in leptotene (a–c), zygotene (d–f), pachytene (g–i and j–k), and diplotene (m–o) stages are shown. RAD21L-positive (g–i) and RAD21L-negative (j–k) pachytene spermatocytes were presumed to be in early pachytene and late pachytene stages, respectively, based on previous reports [17, 18]. The scale bar indicates 10 μm.

that the ratio of RAD21L-positive to meiotic cells (Supplementary Fig. 4) was 99.88% (number of meiotic cells examined = 832), and the percentage of RAD21L-positive cells in the total testicular cells was 44.0%. Thus, 14.5 days after birth, one testis contains 4.15×10^5 meiocytes expressing REC8 and 4.14×10^5 meiocytes expressing RAD21L, on average. Taken together, it is estimated that there are approximately 413,000 RAD21L and 453,000 REC8 molecules per spermatocyte in the early stages (leptotene, zygotene, and pachytene stages) of prophase I.

Discussion

It has been shown that several types of meiotic cohesins are localized along AE/LEs and are essential for chromosomal events that include AE formation, synapsis, recombination, and sister chromatid cohesion in mammals [19, 20, 32]. However, no attempt has been made to determine the intracellular amount of meiotic cohesins. In the present study, for quantitative western blot analysis, we prepared two strains of KI mice that expressed RAD21L-3×FLAG or REC8-3×FLAG as well as recombinant cpREC8-3×FLAG as a standard. After confirming that the 3×FLAG-tagged proteins were expressed and localized in KI mice in essentially the same way as the non-recombinant proteins in wild-type mice (Figs. 2–4), we measured the amount of RAD21L-3×FLAG or REC8-3×FLAG in the testes of 14.5-day-old mice and counted the number of meiotic cells in the testes. Our results demonstrated that there are approximately 413,000 RAD21L and 453,000 REC8 molecules per meiocyte during early prophase I, that is, from the preleptotene stage to mid pachytene stage. Since there is little or no RAD21 in early prophase I [18, 33], the total copy number of cohesin molecules is approximately 866,000 per meiocyte. In contrast to the almost equimolar expression of RAD21L and REC8 in the testes of 14.5-day-old mice, REC8 was much more abundant than RAD21L in the testes of adult mice. This finding is consistent with a previous report that *Rad21L* mRNA levels are much lower than those of *Rec8* in the adult testes [18]. The high expression level of REC8 in the adult testes presumably reflects the higher number of REC8-expressing cells than that of RAD21L-expressing cells because adult testes contain meiocytes (that have crossed the mid-pachytene stage) and post-meiotic cells in which REC8 but not RAD21L is expressed (Fig. 1C).

In a previous study on HeLa cells, using mass spectrometric and fluorescence correlation spectroscopic techniques, approximately 506,000 and 298,000 copies, respectively, per cell of RAD21 (also called SCC1 in the paper) were estimated in the G2 phase, which is

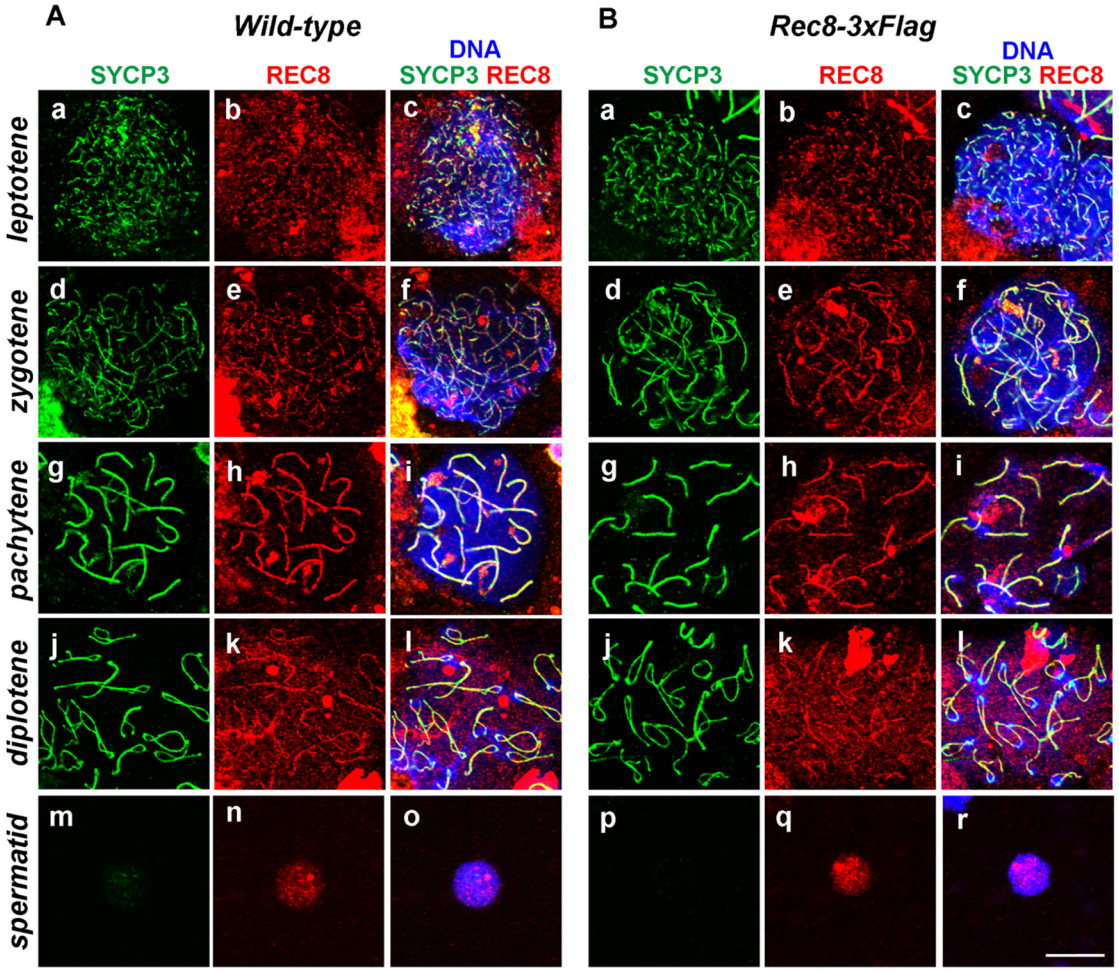

Fig. 4. The localization of REC8 in nuclear spreads from *Rec8-3×Flag* KI and wild-type 8-week-old mice. Nuclear spreads of testicular cells from wild-type (A) and *Rec8-3×Flag* KI (B) 8-week-old mice were prepared and immunofluorescently labelled with anti-RAD21L and anti-SYCP3 antibodies. The DNA was counterstained with DAPI. Spermatocytes in the leptotene (a–c), zygotene (d–f), pachytene (g–i), and diplotene (j–l) stages, as well as spermatids (m–o), are shown. The scale bar indicates 10 µm.

equivalent to prophase I of the meiotic cell cycle [34]. In another study using mouse embryonic stem cells (mESCs) expressing endogenous RAD21 with a Halo-tag, 109,400 RAD21 molecules per cell were estimated [35]. Although it is difficult to make a strict comparison between the amounts of cohesin in mitotic and meiotic cells due to the different methods used in previous studies and the present study, the intracellular amount of cohesin in mouse spermatocytes is 2–3 and 8 times higher than that reported in HeLa cells and mESCs, respectively. Does this high level of cohesin affect the function that cohesin performs in the process of meiosis? Considering that meiotic defects appear only in homozygous mutants deficient for the meiosis-specific cohesin subunit, but not in hetero-deficient mutants, as shown in previous reports [21–23, 36, 37], meiotic cohesin subunits, whose intracellular levels are similar to that of a canonical cohesin subunit reported in HeLa cells, might play important roles in the processes of synapsis and recombination of homologous chromosomes. The proportion of meiotic cohesin that is bound to chromatin cannot be deduced from our experimental results; however, provided that the ratio of cohesin that binds to chromatin is the same in somatic cells and germ cells, it is unlikely that meiosis-specific regulation of chromosome dynamics is caused by the presence of excessive amounts of cohesin in meiotic cells. Nevertheless, it does not rule out the possibility that high levels of cohesin may be useful for some of the processes that occur during meiosis.

It has been shown that AE formation is partially defective in *Smc1β*, *Rec8*, or *Rad21L*-deficient mice [21–23, 36], while AE formation is completely abolished in *Stag3* KO mice [37] or *Rad21L*/*Rec8* double KO mice [24]. It is thought that cohesins create axial cores along chromosomes on which AEs are assembled, because cohesin cores are detectable in *Sycp3* KO spermatocytes [38]. A study using *Rad21L*, *Rec8*, and *Smc1β* single and double KO mice strains suggested that RAD21L-SMC1α-, RAD21L-SMC1β-, and REC8-SMC1β-containing cohesin complexes mainly contribute to regulation of chromosome axis length with some help from SMC1α-REC8-containing cohesins [26]. However, the extent to which RAD21L-containing cohesins and REC8-containing cohesins contribute to AE formation is unknown. Our finding that RAD21L and REC8 were present at an almost equimolar ratio during early prophase I suggests that they contribute equally to AE formation, at least from a quantitative point of view. The architectural role of cohesin has also been observed in mitotically proliferating cells. The cohesin-based chromosome axes, called vermicelli, are also formed in the interphase nucleus when the removal of canonical cohesin from chromosomes is inhibited by Wapl depletion, that is,

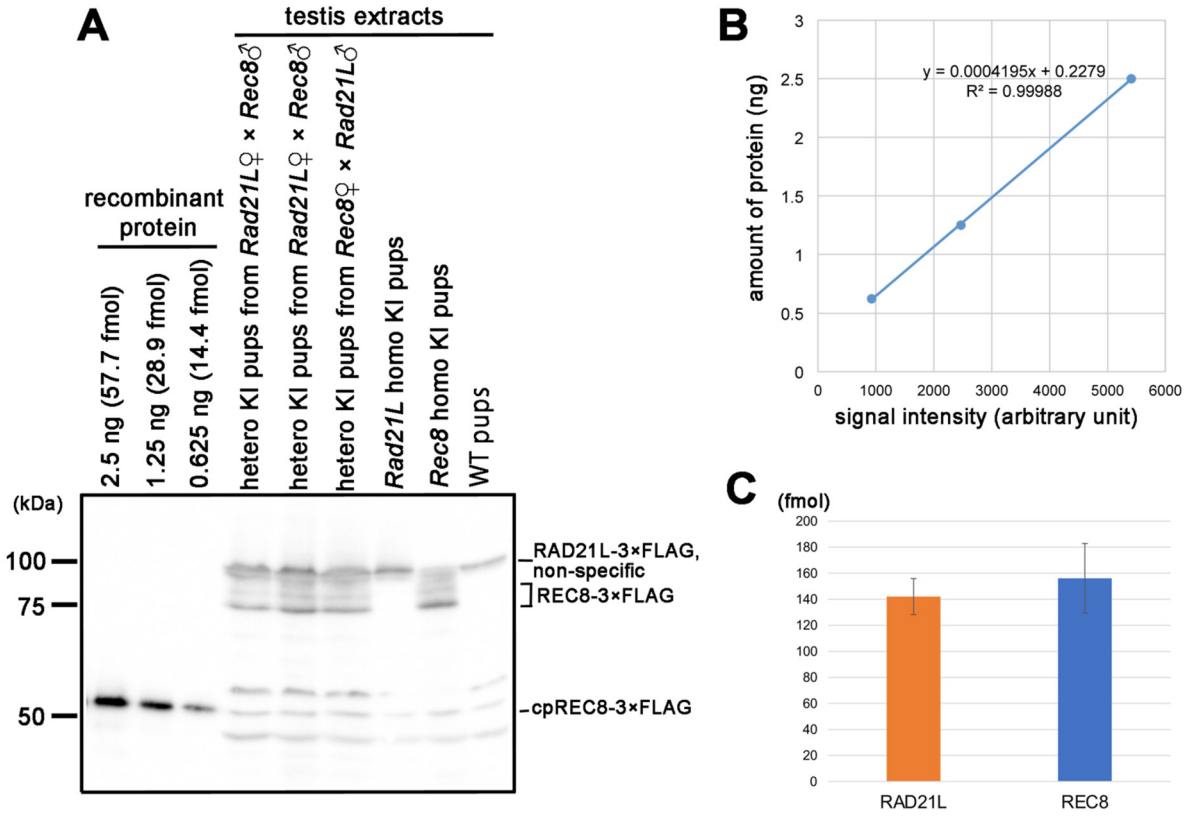

Fig. 5. Quantitative analysis of RAD21L and REC8 in the testes of 14.5-day-old mice. (A) Testis extracts were prepared from 14.5-day-old pups that were born by mating *Rad21L-3×Flag* KI female mice with *Rec8-3×Flag* KI male mice (hetero KI pups from *Rad21L* ♀× *Rec8* ♂), *Rec8-3×Flag* KI female mouse with *Rad21L-3×Flag* KI male mouse (hetero KI pups from *Rec8* ♀× *Rad21L* ♂), female and male *Rad21L-3×Flag* KI mice (*Rad21L* homo KI pups), female and male *Rec8-3×Flag* KI mice (*Rec8* homo KI pups), and female and male wild-type mice (WT pups). One-tenth volumes of the total amounts of testes extracts were loaded in each lane for the hetero KI and WT mice while one-twentieth the amounts were loaded for homo KI mice. The testes extracts were subjected to immunoblot analysis using anti-3×FLAG antibody. Serially diluted recombinant proteins of carboxy terminal partial REC8-3×FLAG (cpREC8) were also separated by SDS-PAGE and subjected to the immunoblot analysis to create a calibration curve. Note that the non-specific band detected using anti-3×FLAG antibody in WT pups partially overlapped with the RAD21L-3×FLAG band. Thus, the signal intensity of RAD21L-3×FLAG was calculated by subtracting the non-specific band intensity from the intensity of the overlapped bands. (B) A calibration curve was made based on the signal intensities of the serially diluted standard samples. The approximation formula and coefficient of determination are also shown. (C) The absolute amounts of RAD21L-3×FLAG and REC8-3×FLAG in a single testis of 14.5-day-old heterozygous KI mouse were calculated based on the signal intensities obtained from three independently prepared samples of hetero KI pups (shown in A) and the calibration curve (shown in B).

when there is a high concentration of cohesins on the chromosomes [39]. Therefore, it is reasonable to consider that cohesin, whether somatic or meiotic, has an intrinsic ability to form chromosomal axial cores, and that this ability may depend, at least in part, on its intracellular amount. In meiotic prophase, topologically associating domains (TADs) are lost as chromosomes are reorganized into linear arrays of chromatin loops anchored to their axial cores [40]. Reorganization of the meiotic chromosome may also be caused, in part, by the high levels of cohesins in meiocytes. This notion is supported by the observation that several major phenotypes of SMC1β-deficient spermatocytes, including axial length shortening, were rescued by SMC1α, which was expressed under the control of the *Smc1β* promotor [41]. Therefore, the quantity rather than the quality of cohesin complexes may be a major determinant of the reorganization of the chromatin axis loop during meiosis.

Genetic analyses using several strains of knockout mice suggested that RAD21L and REC8 have distinctive roles in meiosis; RAD21L contributes to the pairing of homologous chromosomes, while REC8 contributes to sister chromatid cohesion in the early stages of prophase I [25, 42]. However, it is unknown whether the differences in their roles are due to differences in the quality or quantity of these cohesin subunits. Our finding that RAD21L and REC8 were expressed in almost equimolar amounts in the early stages of prophase I refutes the possibility that either one of these proteins is more abundant than the other. Thus, it is reasonable to conclude that the distinctive roles of RAD21L and REC8 suggested in previous genetic studies can be attributed to their unique functions rather than their abundance in the cell.

In summary, this is the first study that revealed the amount of cohesins in mammalian meiocytes, which has provided new insights into the organization of meiotic chromosomes by cohesins in mammalian germ cells: RAD21L and REC8 are expressed at an almost equimolar level during early prophase I. However, the total amount of intracellular cohesins is higher in spermatocytes than that in mammalian somatic cells examined till date. This study also provides useful experimental animal resources for isolation of proteins that interact with meiotic cohesins and investigation of the genomic localization of meiotic cohesins in future studies.

Conflict of interests: The authors declare that there is no conflict in relation to this manuscript.

Acknowledgments

This study was supported in part by JSPS KAKENHI grants (18H02353 and 22K19248) to J.L. This research was also partially supported by the Platform Project for Supporting Drug Discovery and Life Science Research (Basis for Supporting Innovative Drug Discovery and Life Science Research (BINDS)) from AMED under Grant Number JP21am0101120 (support number 0224) to I.H. and T.H.

References

1. **Page SL, Hawley RS.** The genetics and molecular biology of the synaptonemal complex. *Annu Rev Cell Dev Biol* 2004; **20**: 525–558. [Medline] [CrossRef]
2. **Keeney S.** Mechanism and control of meiotic recombination initiation. *Curr Top Dev Biol* 2001; **52**: 1–53. [Medline] [CrossRef]
3. **Gray S, Cohen PE.** Control of meiotic crossovers: From double-strand break formation to designation. *Annu Rev Genet* 2016; **50**: 175–210. [Medline] [CrossRef]
4. **Losada A, Hirano T.** Dynamic molecular linkers of the genome: the first decade of SMC proteins. *Genes Dev* 2005; **19**: 1269–1287. [Medline] [CrossRef]
5. **Peters JM, Tedeschi A, Schmitz J.** The cohesin complex and its roles in chromosome biology. *Genes Dev* 2008; **22**: 3089–3114. [Medline] [CrossRef]
6. **Zhang N, Kuznetsov SG, Sharan SK, Li K, Rao PH, Pati D.** A handcuff model for the cohesin complex. *J Cell Biol* 2008; **183**: 1019–1031. [Medline] [CrossRef]
7. **Nasmyth K, Haering CH.** Cohesin: its roles and mechanisms. *Annu Rev Genet* 2009; **43**: 525–558. [Medline] [CrossRef]
8. **Stigler J, Çamdere GÖ, Koshland DE, Greene EC.** Single-molecule imaging reveals a collapsed conformational state for dna-bound cohesin. *Cell Reports* 2016; **15**: 988–998. [Medline] [CrossRef]
9. **Rao SSP, Huang SC, Glenn St Hilaire B, Engreitz JM, Perez EM, Kieffer-Kwon KR, Sanborn AL, Johnstone SE, Bascom GD, Bochkov ID, Huang X, Shamim MS, Shin J, Turner D, Ye Z, Omer AD, Robinson JT, Schlick T, Bernstein BE, Casellas R, Lander ES, Aiden EL.** Cohesin loss eliminates all loop domains. *Cell* 2017; **171**: 305–320.e24. [Medline] [CrossRef]
10. **Schwarzer W, Abdennur N, Goloborodko A, Pekowska A, Fudenberg G, Loe-Mie Y, Fonseca NA, Huber W, Haering CH, Mirny L, Spitz F.** Two independent modes of chromatin organization revealed by cohesin removal. *Nature* 2017; **551**: 51–56. [Medline] [CrossRef]
11. **Wutz G, Várnai C, Nagasaka K, Cisneros DA, Stocsits RR, Tang W, Schoenfelder S, Jessberger G, Muhar M, Hossain MJ, Walther N, Koch B, Kueblbeck M, Ellenberg J, Zuber J, Fraser P, Peters JM.** Topologically associating domains and chromatin loops depend on cohesin and are regulated by CTCF, WAPL, and PDS5 proteins. *EMBO J* 2017; **36**: 3573–3599. [Medline] [CrossRef]
12. **Revenkova E, Eijpe M, Heyting C, Gross B, Jessberger R.** Novel meiosis-specific isoform of mammalian SMC1. *Mol Cell Biol* 2001; **21**: 6984–6998. [Medline] [CrossRef]
13. **Prieto I, Suja JA, Pezzi N, Kremer L, Martínez-A C, Rufas JS, Barbero JL.** Mammalian STAG3 is a cohesin specific to sister chromatid arms in meiosis I. *Nat Cell Biol* 2001; **3**: 761–766. [Medline] [CrossRef]
14. **Eijpe M, Offenberg H, Jessberger R, Revenkova E, Heyting C.** Meiotic cohesin REC8 marks the axial elements of rat synaptonemal complexes before cohesins SMC1beta and SMC3. *J Cell Biol* 2003; **160**: 657–670. [Medline] [CrossRef]
15. **Lee J, Iwai T, Yokota T, Yamashita M.** Temporally and spatially selective loss of Rec8 protein from meiotic chromosomes during mammalian meiosis. *J Cell Sci* 2003; **116**: 2781–2790. [Medline] [CrossRef]
16. **Gutiérrez-Caballero C, Herrán Y, Sánchez-Martín M, Suja JA, Barbero JL, Llano E, Pendás AM.** Identification and molecular characterization of the mammalian α-kleisin RAD21L. *Cell Cycle* 2011; **10**: 1477–1487. [Medline] [CrossRef]
17. **Ishiguro K, Kim J, Fujiyama-Nakamura S, Kato S, Watanabe Y.** A new meiosis-specific cohesin complex implicated in the cohesin code for homologous pairing. *EMBO Rep* 2011; **12**: 267–275. [Medline] [CrossRef]
18. **Lee J, Hirano T.** RAD21L, a novel cohesin subunit implicated in linking homologous chromosomes in mammalian meiosis. *J Cell Biol* 2011; **192**: 263–276. [Medline] [CrossRef]
19. **Lee J.** Chapter 15: The regulation and function of cohesin and condensin in mammalian oocytes and spermatocytes. In: Kloc M (ed.), Oocytes -Maternal information and functions, Springer, Results and Problems in Cell Differentiation. 2017; **63**: 355–372.
20. **Ishiguro KI.** The cohesin complex in mammalian meiosis. *Genes Cells* 2019; **24**: 6–30. [Medline] [CrossRef]
21. **Bannister LA, Reinholdt LG, Munroe RJ, Schimenti JC.** Positional cloning and characterization of mouse mei8, a disrupted allelle of the meiotic cohesin Rec8. *Genesis* 2004; **40**: 184–194. [Medline] [CrossRef]
22. **Xu H, Beasley MD, Warren WD, van der Horst GT, McKay MJ.** Absence of mouse REC8 cohesin promotes synapsis of sister chromatids in meiosis. *Dev Cell* 2005; **8**: 949–961. [Medline] [CrossRef]
23. **Herrán Y, Gutiérrez-Caballero C, Sánchez-Martín M, Hernández T, Viera A, Barbero JL, de Álava E, de Rooij DG, Suja JA, Llano E, Pendás AM.** The cohesin subunit RAD21L functions in meiotic synapsis and exhibits sexual dimorphism in fertility. *EMBO J* 2011; **30**: 3091–3105. [Medline] [CrossRef]
24. **Llano E, Herrán Y, García-Tuñón I, Gutiérrez-Caballero C, de Álava E, Barbero JL, Schimenti J, de Rooij DG, Sánchez-Martín M, Pendás AM.** Meiotic cohesin complexes are essential for the formation of the axial element in mice. *J Cell Biol* 2012; **197**: 877–885. [Medline] [CrossRef]
25. **Ishiguro K, Kim J, Shibuya H, Hernández-Hernández A, Suzuki A, Fukagawa T, Shioi G, Kiyonari H, Li XC, Schimenti J, Höög C, Watanabe Y.** Meiosis-specific cohesin mediates homolog recognition in mouse spermatocytes. *Genes Dev* 2014; **28**: 594–607. [Medline] [CrossRef]
26. **Biswas U, Wetzker C, Lange J, Christodoulou EG, Seifert M, Beyer A, Jessberger R.** Meiotic cohesin SMC1β provides prophase I centromeric cohesion and is required for multiple synapsis-associated functions. *PLoS Genet* 2013; **9**: e1003985. [Medline] [CrossRef]
27. **Vara C, Paytuví-Gallart A, Cuartero Y, Le Dily F, Garcia F, Salvà-Castro J, Gómez-H L, Julià E, Moutinho C, Aiese Cigliano R, Sanseverino W, Fornas O, Pendás AM, Heyn H, Waters PD, Marti-Renom MA, Ruiz-Herrera A.** Three-dimensional genomic structure and cohesin occupancy correlate with transcriptional activity during spermatogenesis. *Cell Reports* 2019; **28**: 352–367.e9. [Medline] [CrossRef]
28. **Horii T, Morita S, Kimura M, Terawaki N, Shibutani M, Hatada I.** Efficient generation of conditional knockout mice via sequential introduction of lox sites. *Sci Rep* 2017; **7**: 7891. [Medline] [CrossRef]
29. **Heyting C, Dietrich AJ.** Meiotic chromosome preparation and protein labeling. *Methods Cell Biol* 1991; **35**: 177–202. [Medline] [CrossRef]
30. **Bellvé AR, Cavicchia JC, Millette CF, O'Brien DA, Bhatnagar YM, Dym M.** Spermatogenic cells of the prepuberal mouse. Isolation and morphological characterization. *J Cell Biol* 1977; **74**: 68–85. [Medline] [CrossRef]
31. **Drumond AL, Meistrich ML, Chiarini-Garcia H.** Spermatogonial morphology and kinetics during testis development in mice: a high-resolution light microscopy approach. *Reproduction* 2011; **142**: 145–155. [Medline] [CrossRef]
32. **Grey C, de Massy B.** Chromosome organization in early meiotic prophase. *Front Cell Dev Biol* 2021; **9**: 688878. [Medline] [CrossRef]
33. **Prieto I, Pezzi N, Buesa JM, Kremer L, Barthelemy I, Carreiro C, Roncal F, Martínez A, Gómez L, Fernández R, Martínez-A C, Barbero JL.** STAG2 and Rad21 mammalian mitotic cohesins are implicated in meiosis. *EMBO Rep* 2002; **3**: 543–550. [Medline] [CrossRef]
34. **Holzmann J, Politi AZ, Nagasaka K, Hantsche-Grininger M, Walther N, Koch B, Fuchs J, Dürnberger G, Tang W, Ladurner R, Stocsits RR, Busslinger GA, Novák B, Mechtler K, Davidson IF, Ellenberg J, Peters JM.** Absolute quantification of cohesin, CTCF and their regulators in human cells. *eLife* 2019; **8**: e46269. [Medline] [CrossRef]
35. **Cattoglio C, Pustova I, Walther N, Ho JJ, Hantsche-Grininger M, Inouye CJ, Hossain MJ, Dailey GM, Ellenberg J, Darzacq X, Tjian R, Hansen AS.** Determining cellular CTCF and cohesin abundances to constrain 3D genome models. *eLife* 2019; **8**: e40164. [Medline] [CrossRef]
36. **Revenkova E, Eijpe M, Heyting C, Hodges CA, Hunt PA, Liebe B, Scherthan H, Jessberger R.** Cohesin SMC1 beta is required for meiotic chromosome dynamics, sister chromatid cohesion and DNA recombination. *Nat Cell Biol* 2004; **6**: 555–562. [Medline] [CrossRef]
37. **Winters T, McNicoll F, Jessberger R.** Meiotic cohesin STAG3 is required for chromosome axis formation and sister chromatid cohesion. *EMBO J* 2014; **33**: 1256–1270. [Medline] [CrossRef]
38. **Pelttari J, Hoja M-R, Yuan L, Liu JG, Brundell E, Moens P, Santucci-Darmanin S, Jessberger R, Barbero JL, Heyting C, Höög C.** A meiotic chromosomal core consisting of cohesin complex proteins recruits DNA recombination proteins and promotes synapsis in the absence of an axial element in mammalian meiotic cells. *Mol Cell Biol* 2001; **21**: 5667–5677. [Medline] [CrossRef]
39. **Tedeschi A, Wutz G, Huet S, Jaritz M, Wuensche A, Schirghuber E, Davidson IF, Tang W, Cisneros DA, Bhaskara V, Nishiyama T, Vaziri A, Wutz A, Ellenberg J, Peters J-M.** Wapl is an essential regulator of chromatin structure and chromosome segregation. *Nature* 2013; **501**: 564–568. [Medline] [CrossRef]
40. **Patel L, Kang R, Rosenberg SC, Qiu Y, Raviram R, Chee S, Hu R, Ren B, Cole F, Corbett KD.** Dynamic reorganization of the genome shapes the recombination landscape in meiotic prophase. *Nat Struct Mol Biol* 2019; **26**: 164–174. [Medline] [CrossRef]
41. **Biswas U, Stevense M, Jessberger R.** SMC1 alpha substitutes for many meiotic functions of SMC1beta but cannot protect telomeres from damage. *Curr Biol* 2018; **28**: 249–261.e4. [Medline] [CrossRef]
42. **Agostinho A, Manneberg O, van Schendel R, Hernández-Hernández A, Kouznetsova A, Blom H, Brismar H, Höög C.** High density of REC8 constrains sister chromatid axes and prevents illegitimate synaptonemal complex formation. *EMBO Rep* 2016; **17**: 901–913. [Medline] [CrossRef]